Detection of thin cirrus from 1.38 μm/0.65 μm reflectance ratio combined with 8.6–11 μm brightness temperature difference

J. K. Roskovensky and K. N. Liou

Dept. of Atmospheric Sciences, Univ. of California, Los Angeles, California, USA

Received 9 July 2003; revised 12 August 2003; accepted 3 September 2003; published 7 October 2003.

[1] We developed a new detection scheme for the identification of thin cirrus based on a combination of the 1.38 μm and 0.65 μm reflectance ratio and 8.6–11 μm brightness temperature difference. Results computed from a radiative transfer model as well as data obtained from the Moderate Resolution Imaging Spectroradiometer (MODIS) onboard the Terra satellite were used to demonstrate the applicability of this method for regional mapping of thin cirrus. The mm-wave radar backscatter data, coincident and collocated with MODIS data, available from the DOE's Atmospheric Radiation Measurement (ARM) sites, was employed for validation of the present satellite detection results. In all cases selected, our new method was able to detect the majority of thin cirrus estimated to have optical thickness between 0.1 and 0.9. It also compared favorably to existing detection tests. *INDEX TERMS:* 3359 Meteorology and Atmospheric Dynamics: Radiative processes; 3360 Meteorology and Atmospheric Dynamics: Remote sensing; 3394 Meteorology and Atmospheric Dynamics: Instruments and techniques. **Citation:** Roskovensky, J. K., and K. N. Liou, Detection of thin cirrus from 1.38 μm/0.65 μm reflectance ratio combined with 8.6–11 μm brightness temperature difference, *Geophys. Res. Lett.*, *30*(19), 1985, doi:10.1029/2003GL018135, 2003.

1. Introduction

[2] Cloud contamination remains a major problem and a leading source of error [*Mishchenko et al.*, 1999] when retrieving aerosol and surface properties from satellites. Accurate cloud screening to determine cloud-free pixels is essential. The techniques using spatial variance tests differentiate clouds from aerosols over the oceans [*Coakley and Bretherton*, 1982; *Martins et al.*, 2002]. However, these techniques often fail to detect thin homogeneous cirrus and cannot be employed safely over land surfaces due to the large variation in albedo. The use of the 1.38 μm band has been identified as a viable cirrus cloud detection tool [*Gao and Kaufman*, 1995]. Due to the existence of a strong water vapor absorption band near 1.38 μm and the fact that nearly all of the atmospheric water vapor exists below the cirrus level, reflectance from the MODIS 1.38 μm channel is produced primarily by high clouds [*Gao et al.*, 2003]. As a result, 1.38 μm reflectance can be used in a ratio with a non-absorbing band to discriminate thin cirrus from aerosols. *Gao et al.* [2002] differentiated dust from cirrus using the 1.38 μm/1.24 μm reflectance ratio with a threshold value of 0.3. We find that this approach may not be sufficiently robust to detect thin cirrus with optical depth less than 0.5 and may produce ambiguity in differentiating clear ocean pixels from those of thin cirrus. To complement the preceding approach, we developed a new thin cirrus detection scheme using the 1.38 μm/0.65 μm reflectance ratio and the 8.6 and 11 μm brightness temperature difference (BTD). Since each test is sensitive to a particular cirrus trait, 1.38 μm reflectance to the altitude and thickness and the BTD to the ice phase, the two tests work together well to produce a more powerful cirrus detection parameter. At the same time, because both tests can also be sensitive to dust in a dry atmosphere, we will confine our study to non-dust situations which represent the vast majority of cases pertaining to the regions examined here. However, adjustments to our algorithm can be made for the detection of dust. We chose the 0.65 μm band over the 1.24 μm band solely because, when used in ratio with the 1.38 μm band, it can differentiate cirrus from aerosols more clearly over the ocean, where 1.24 μm reflectance can be exceedingly small. We perform theoretical calculations to investigate the sensitivity of the new scheme and use MODIS data over both a land and an ocean ARM site where mm-wave radar data is available to verify satellite detection results. In addition, we compare our cirrus detection results to those of existing algorithms.

0094-8276/03/2003GL018135$05.00

2. New Cirrus Masking Technique

[3] Radiative transfer calculations were carried out for both cirrus and aerosol atmospheres using the adding/doubling method and employing nonspherical randomly oriented ice crystals [*Takano and Liou*, 1989b]. For the thermal infrared wavelengths, single scattering calculations were performed using randomly oriented prolate spheroids and hexagonal crystals through parameterization based on the anomalous diffraction theory and geometric ray-tracing [*Takano et al.*, 1992]. The simulated ice cloud was 2 km thick with cloud top at 10 km and possessed a particle size distribution described in *Heymsfield and Platt* [1984] and *Takano and Liou* [1989a] with a mean effective ice crystal size of 24 μm, as defined in equation (3) in *Rolland et al.* [2000]. The aerosol distribution used was that described as clean-continental in *D'Almeida et al.* [1991]. Figures 1a and 1b show the modeled 1.38 μm/1.24 μm and 1.38 μm/0.65 μm reflectance ratios, respectively, for two different viewing geometries versus cirrus and aerosol optical depths. The solid curves represent cirrus with both the solar and satellite viewing angles of 10° and the dashed curves with both angles of 50°, each using a relative azimuthal angle of 135°. The dotted curves represent aerosols with the same geometry. It can be seen that these reflectance ratios (RR) may only detect cirrus with optical depths as low as 0.4

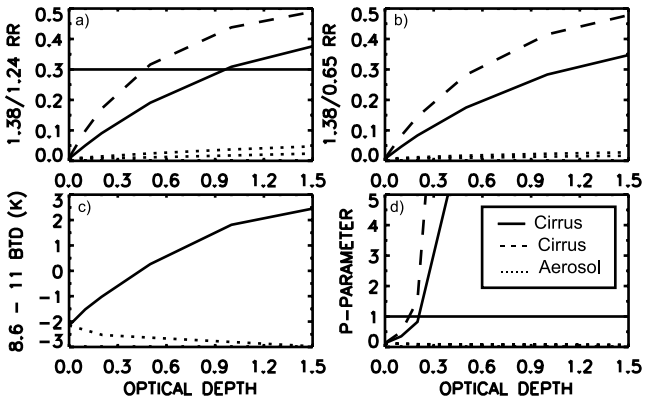

Figure 1. Theoretical calculations of the (a) 1.38 μm/1.24 μm reflectance ratio, (b) 1.38 μm/0.65 μm reflectance ratio, (c) 8.6–11 μm BTD, and (d) cirrus detection P-parameter as a function of cirrus and aerosol optical depth over a land surface with albedo of 10%.

(using a threshold value of 0.3) for the more reflective geometry (dashed curve) and that the detectable limit may be as high as 1 (solid curve). Figure 1c shows how 8.6–11 μm BTD increases with cirrus optical depth since ice is more absorbing at 11 μm than at 8.6 μm [*Menzel et al.*, 2002]. Both the RR and BTD values increase slowly with increasing cirrus optical depth. Taking advantage of this relationship, we developed the high cloud screening parameter (P), which combines the RR and BTD as follows:

$$P = \exp[RR^{*}A + (BTD - B)], \quad (1)$$

where RR represents the 1.38 μm/0.65 μm reflectance ratio and A is its scaling factor and B is the BTD offset. Figure 1d shows how fast this exponential function P increases for cirrus clouds and that, by using a threshold value of 1 (zero exponent) and 10 and 0 for A and B, respectively, cirrus with optical depths less than 0.2 may be detected. Also, the radiative transfer calculations show that P values decrease with increasing aerosol optical depth due to the influence of the BTD, while RR values increase. This makes the P-parameter less likely to mistake a thick non-dust aerosol layer with thin cirrus. For dust in a dry atmosphere, radiative transfer calculations show that the A and B values must be changed to approximately 6 and −2, respectively, in order to prohibit dust from being detected as cirrus. This also has the effect of reducing the P-parameters theoretical cirrus detection capability to a minimum cloud optical depth of 0.4.

[4] Since modeled clear sky BTD values lie near −2 K, yet observed clear sky BTD values can vary substantially from scene to scene, we introduce the B offset defined as $B = M_{BTDclr} + \sigma_{BTDclr} + 2$, where M represents the mean clear sky BTD and σ is the standard deviation of the clear sky BTD pixels. This parameterization eliminates scene-by-scene variation in BTD and sets up a mini-threshold for cirrus (one standard deviation above the mean clear sky value) and scales the cirrus threshold in the second term of Equation 1 to −2 K. As a result, the mini-threshold for cirrus in the first exponential term of Equation 1 should be 2 so that cirrus pixels will make the overall exponent value in this equation positive. The following parameterization fulfills this requirement. $A = 2/(M_{RRclr} + \sigma_{RRclr})$. In this manner, pixels with RR values that make the first term in equation (1) less than 2 can still be classified as thin cirrus as long as their BTD values are large enough to compensate, and vice versa. Due to the highly sensitive nature of RR to surface reflectance and BTD to surface temperature, cloud emisivity, and atmospheric water vapor concentrations, values of A and B must be determined from nearby clear sky values (i. e. within the same MODIS granule). Using only two land and three ocean MODIS granules, identified in the following section, we have found mean clear sky RR values of 0.12 and 0.23 requiring mean scaling factors, A, to be 13.2 and 8.66 for land and ocean surfaces, respectively. Mean clear sky BTD values, which varied by more than 1 K from scene to scene, were −2.7 K and −2.1 K and resulted in B offsets of −0.24 K and 0.44 K for land and ocean, respectively.

[5] Observed RR, A, BTD, and B values for an ocean scene are shown as a function of satellite scan angle in Figure 2 (a–d), respectively. The solid curves represent clear sky pixels defined as having a clear sky probability over 95% (MODIS cloud mask MOD35 product, *Ackerman et al.* [2002]), 1.38 μm reflectance below 1.1% and 8.6–11 μm BTD under −0.5 K. The other curves are presumed to represent thin cirrus because they possess low visible reflectance (less than 20%) and 1.38 μm reflectance above the average clear sky threshold (mean value plus one standard deviation). The dotted, dashed and alternating dashed-dotted curves represent pixels with 1.38 μm reflectance between 1.1%–1.5%, 1.5%–2%, and above 2%, respectively. By using clear sky values for RR and BTD, A and B values were determined such that clear sky, aerosol filled and low cloud pixels possess P values that lie just below the P threshold of 1 as demonstrated in Figure 2e. Therefore, cirrus filled pixels lie above the threshold. Due to

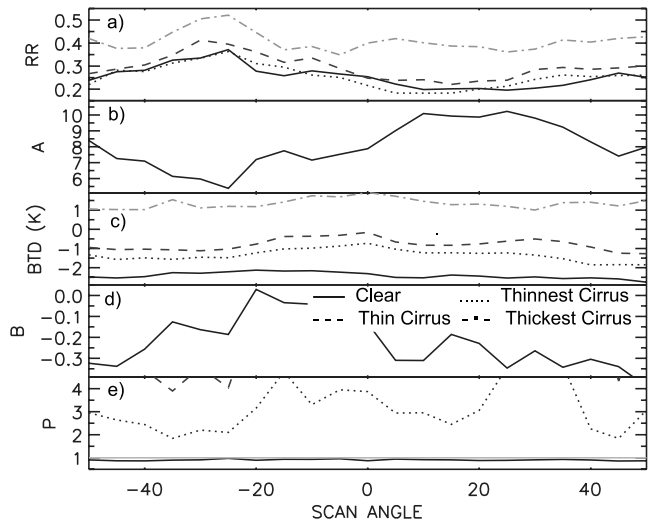

Figure 2. Observed MODIS/Terra (a) 1.38 μm/0.65 μm reflectance ratio and (c) 8.6–11 μm brightness temperature difference as a function of satellite viewing angle for the ocean case of November 14, 2001(2340 UTC). Also given are the calculated A, B, and P parameters, as described in the text, in (b), (d) and (e), respectively.

Table 1. Comparisons of Satellite and mm-Wave Radar Cirrus Detection[a]

Parameter	11 February (1730Z)	22 March (1735Z)	16 August (2310Z)	14 November (2340Z)	18 November (2315Z)
Radar Cirrus Cloud (%)	100	100	100	94	87
Cloud Thickness range (km)	0.5–1.5	0.7–2.8	0.1–2.2	0.1–1.2	0.1–1.5
Maximum Cloud Top (km)	10.7	10.6	10.3	14.3	13.2
Cirrus Optical Depth range	0.1–0.5	0.15–0.9	0.02–0.7	0.02–0.36	0.02–0.46
Cirrus Detection Results	11 February	22 March	16 August	14 November	18 November
P-parameter[b]	86	87	100	80	83
1.38/1.24 Ratio[c]	0	0	81	44	64
3 × 3 SD[d]	na	Na	94	78	85

[a]Empirical optical depths were calculated using theoretical extinction coefficients produced for ice crystals with effective sizes of 10 and 42 μm [*Liou*, 2002]. Numerical values in the bottom section are listed in percent.
[b]New cirrus detection parameter.
[c]Cirrus detection algorithm of *Gao et al.* [2002].
[d]Cloud detection algorithm of *Martins et al.* [2002].

low clear sky 0.65 μm reflectance over the ocean, the RR values for the thinnest cirrus (dotted curve) are very similar to that of clear sky values. This is not the case for the BTD clear sky and thin cirrus values shown in Figure 2c. As a result, for ocean scenes σ_{RRclr} is set to 0 and $2\sigma_{BTDclr}$ is used in place of σ_{BTDclr}. This is not necessary for land scenes since the distinction between thin cirrus and clear sky RR values is clear. Notice how A is inversely proportional to the clear sky RR values and that the sunglint region between −20° and 45°, where RR is decreased due to increased 0.65 μm reflection, is taken into account without effecting the results for the P-parameter. Besides larger clear sky values, reflectance ratio values of 1.38 μm/1.24 μm were similar to those of 1.38 μm/0.65 μm for this case.

3. Results

[6] MODIS data over the two ARM sites of the Southern Great Plains (SGP, land) and the Tropical Western Pacific (TWP, ocean), near the island Republic of Nauru, was examined because each site possesses a mm-wave radar useful in verifying the presence of thin cirrus. Five MODIS granules from 2001 were identified by the radars as having extensive thin cirrus coverage without a major presence of other clouds during a 1-hour period centered on a MODIS/Terra overpass. The specific cirrus cloud properties as determined from radar reflectivity are presented in the top section of Table 1. The first two cases are from the SGP site, while the remaining three are from the TWP site. The bottom section of Table 1 shows the agreement (in percentage) between the radar and the satellite cirrus detection results. Besides the P-parameter method, we have also calculated results from the 1.38 μm/1.24 μm reflectance ratio test with a 0.3 cirrus threshold, hereafter named 1.38/1.24 ratio, described in *Gao et al.* [2002], and the spatial variability test of *Martins et al.* [2002], hereafter referred to as the 3 × 3 SD method. The latter test uses 0.55 μm reflectance standard deviation from a 3 × 3 pixel region and a threshold value of 0.0025 to detect any type of cloud over ocean. In order to validate the satellite cirrus detection results we match the nine nearest (3 × 3) pixels in space to points in the radar time series at 2-minute intervals using the cirrus level wind beginning 30 minutes before the MODIS overpass and ending 30 minutes afterward. This provided a total of 279 comparisons for each case.

[7] The mm-wave radar detected thin cirrus over both of the land scenes 100% of the time. The P-parameter was able to detect over 86% of the cloud in these two cases while the 1.38/1.24 ratio was unable to detect any of this thin cirrus calculated as having optical depth well below 0.9. This indicates that the threshold presented in *Gao et al.* [2002] may not be optimal for detecting very thin cirrus in non-dust cases. Figures 3b and 3c show that the 1.38 μm reflectance and the 8.6–11 μm BTD generally correlate with the radar reflectivity time series (Figure 3a) for the February 11 case, given that the cirrus level wind was nearly entirely westerly in nature. The radar time series is given backward so that so that the earliest time matches the spatial location at the right sides of the other plots while the latest time matches the left sides. The P-parameter results (Figure 3d) show that nearly all of the thin cirrus was detected except some of the earlier cloud associated with both low 1.38 μm reflectance and 8.6–11 μm BTD located to the east of the radar (36.6°N, 97.5°W).

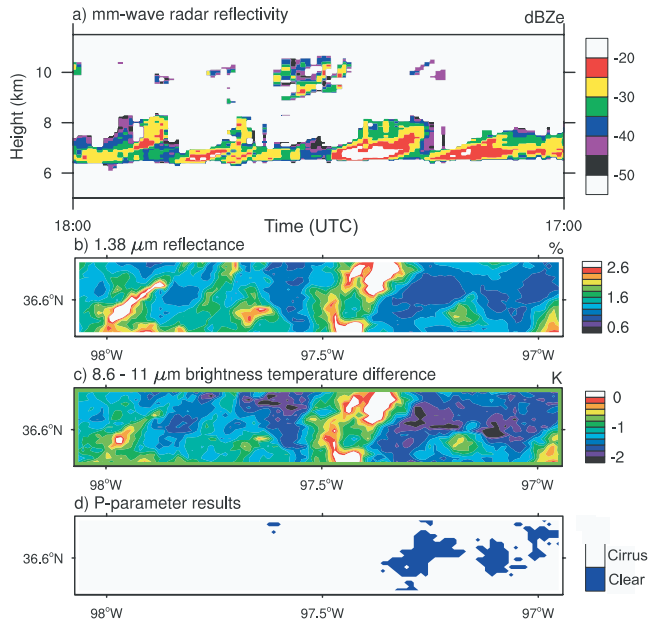

Figure 3. A case study from the SGP-ARM site on February 11, 2001(1730 UTC) is presented. Plotted in (a) is the 1-hour mm-wave radar reflectivity time series from Lamont, OK. The MODIS/Terra 1.38 μm reflectance and 8.6–11 μm BTD are displayed in (b) and (c), respectively, while (d) shows the cirrus detection P-parameter results.

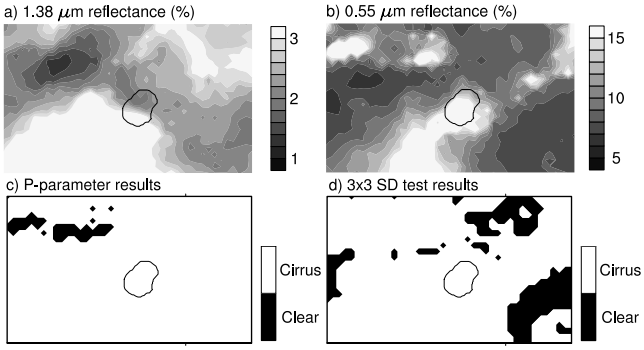

Figure 4. A case study from a 25 × 40 km section centered on the island Republic of Nauru in the TWP-ARM site on November 14, 2001(2343 UTC). Plotted are the (a) MODIS/Terra 1.38 μm reflectance and (b) 0.55 μm reflectance, (c) P-parameter results, and (d) 3 × 3 SD results.

[8] Results from Table 1 indicate that the P-parameter and the 3 × 3 SD tests did better at detecting the thin cirrus over ocean than the 1.38/1.24 ratio. The 1.38 μm reflectance, 0.55 μm reflectance, P-parameter and 3 × 3 SD results are presented for a small region surrounding the island Republic of Nauru in Figure 4 (a–d), respectively. Since cirrus optical depth is proportional to 1.38 μm reflectance, it is apparent that the thinnest cloud is located northwest of the island. The P-parameter clear sky regions correlate well with the low 1.38 μm reflectance despite the appearance of regions of high 0.55 μm reflectance indicative of thick low cloud. This clearly shows that the P-parameter is not sensitive to low-level clouds as expected. The 3 × 3 SD clear sky areas, on the other hand, do not correlate with low 1.38 μm reflectance or to the P-parameter clear sky regions. In fact, some of the 3 × 3 SD clear patches, located northeast of the island, occur where the 1.38 μm reflectance is relatively high and thus where a cirrus cloud is most likely to be present. This test will mark homogenous visible reflective cloud regions as clear. Thus, despite the nearly equal correlation of both tests to the complete radar time series, the spatial results of the P-parameter and the 3 × 3 SD tests do not agree, because the P-parameter only detects high cloud while the 3 × 3 SD detects any cloud that produce substantial variance in visible reflectance. As a result, these two schemes seem to complement each other well in detecting all existing cloud types over the ocean.

[9] Not presented here are histograms of the three cloud screening test values from observed clear sky and cirrus pixels with calculated optical depths less than 0.5 over both land and ocean. Only the P-parameter adequately separated clear sky pixels from the thin cirrus pixels over both land and ocean. The 1.38 μm/1.24 μm ratio threshold of 0.3 was too high to identify any cirrus over land since the mean cirrus ratio value of 0.12 was well under the threshold. For these data, the clear sky ocean 1.38 μm/1.24 μm ratio values were nearly three times greater than the cirrus values and were, consequently, all classified as cirrus. This was due mostly to extremely low 1.24 μm reflectance observed off the ocean. A small fraction of the mm-wave radar detected cirrus pixels over the ocean (5–10%) were identified as clear sky, even by the P-parameter approach, indicating that some of the thinnest cirrus may be still indistinguishable from the background.

4. Conclusion

[10] Using the 1.38 μm/visible reflectance ratio along with the 8.6–11 μm BTD, a new cloud screening parameter (P) was developed which appears to detect thin cirrus well over both land and ocean surfaces for non-dust cases. Modeled radiative transfer calculations indicate that the P-parameter may be sensitive to thin cirrus with visible optical depths on the order of 0.1. Five specific MODIS cases were studied which showed that the P-parameter was able to identify between 80–100% of the thin cirrus calculated to posses optical depths below 0.5. Its use over land can benefit aerosol retrievals because spatial variation tests cannot be employed and the 1.38 μm reflectance ratios alone may not be sufficiently sensitive to detect very thin cirrus clouds. The different spatial distributions of the P-parameter and the visible reflectance spatial variance results shows that each test is measuring a very different quality of the atmosphere/cloud system and that employing both tests can lead to enhanced cloud detection over ocean. Finally, it should be pointed out that the P-parameters effectiveness in dust filled scenes is a subject requiring further investigation.

[11] **Acknowledgments.** We obtained MODIS data from the NASA GES DAAC center and millimeter-wave radar reflectivity data from the Univ. of Utah website. This research was supported by DOE grant DE-FG03-00ER62904, JPL/NASA grant 1241575, and AFOSR grant F49620-01-1-0057.

References

Ackerman, S. A., K. I. Strabala, W. P. Menzel, R. Frey, C. Moeller, L. Gumley, B. A. Baum, S. W. Seeman, and H. Zhang, Discriminating clear-sky from cloud with MODIS algorithm theoretical basis document (MOD35), in *ATBD-MOD-06*, Version 4.0, 115 pp, NASA, Greenbelt, MD, 2002. (available as http://modis.gsfc.nasa.gov/data/atbd/atbd_mod06.pdf)

Coakley, J. A., and F. P. Bretherton, Cloud cover from high-resolution scanner data: Detecting and allowing for partially filled fields of view, *J. Geophys. Res.*, *87*, 4917–4932, 1982.

D'Almeida, G., P. Koepke, and E. Shettle, *Atmospheric aerosols: Global climatology and radiative characteristics*, 561 pp., A. Deepak, Hampton, VA, 1991.

Gao, B. C., and Y. Kaufman, Selection of the 1.375-μm MODIS channel for remote sensing of cirrus clouds and stratospheric aerosols from space, *J. Atmos. Sci.*, *52*, 4231–4237, 1995.

Gao, B. C., Y. Kaufman, D. Tanre, and R. R. Li, Distinguishing tropospheric aerosols from thin cirrus clouds for improved aerosol retrievals using the ratio of 1.38-μm and 1.24-μm channels, *Geophy. Res. Lett.*, *29*(18), 1890, doi:10.1029/2002GL0015475, 2002.

Gao, B. C., P. Yang, and R. R. Li, Detection of high clouds in polar regions during the daytime using the MODIS 1.375-μm channel, *IEEE trans. Geosci. Remote Sens.*, *41*, 474–481, 2003.

Heymsfield, A. J., and C. M. R. Platt, A parameterization of the particle size spectrum of ice clouds in terms of the ambient temperature and the ice water content, *J. Atmos. Sci.*, *41*, 846–855, 1984.

Liou, K. N., *An Introduction to Atmospheric Radiation*, 2nd ed., 583 pp., Academic Press, San Diego, CA, 2002.

Martins, J. V., L. Remer, Y. Kaufman, S. Mattoo, and R. Levy, MODIS cloud screening for remote sensing of aerosols over oceans using spatial variability, *Geophy. Res. Lett.*, *29*(12), 8009, doi:10.1029/2001GL013252, 2002.

Menzel, W. P., B. A. Baum, K. I. Strabala, and R. A. Frey, Cloud top properties and cloud phase algorithm theoretical basis document, in *ATBD-MOD-04*, Version 6.0, 62 pp, NASA, Greenbelt, MD, 2002. (available as http://modis.gsfc.nasa.gov/atbd/atbd_mod04.pdf)

Mishchenko, M. I., I. V. Geogdzhayev, B. Cairns, W. B. Rossow, and A. A. Lacis, Aerosol retrievals over the ocean by use of channels 1 and 2

AVHRR data: Sensitivity analysis and preliminary results, *Appl. Opt.*, *38*, 7325–7341, 1999.

Rolland, P., K. N. Liou, M. D. King, S. C. Tsay, and G. M. McFarquhar, Remote sensing of optical and microphysical properties of cirrus clouds using Moderate-Resolution Imaging Spectroradiometer channels: Methodology and sensitivity to physical assumptions, *J. Geophys. Res.*, *105*, 11,721–11,738, 2000.

Takano, Y., and K. N. Liou, Solar radiative transfer in cirrus clouds. Part I: Single-scattering and optical properties of hexagonal ice crystals, *J. Atmos. Sci.*, *46*, 3–19, 1989a.

Takano, Y., and K. N. Liou, Solar radiative transfer in cirrus clouds. Part II: Theory and computation of multiple scattering in an anisotropic medium, *J. Atmos. Sci.*, *46*, 20–36, 1989b.

Takano, Y., K. N. Liou, and P. Minnis, The effects of small ice crystals on cirrus infrared radiative properties, *J. Atmos. Sci.*, *49*, 1487–1493, 1992.

J. K. Roskovensky and K. N. Liou, Dept. of Atmospheric Sciences, Univ. of California, Los Angeles, CA USA. (jrosko@atmos.ucla.edu)